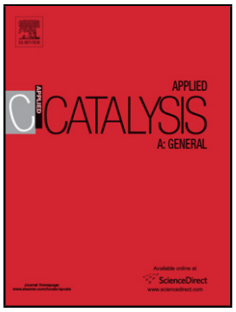

Title: Stilbene synthesis through decarboxylative
cross-coupling of substituted cinnamic acids with aryl halides

Authors: Nelly Rameau, Baptiste Russo, Stéphane
Mangematin, Catherine Pinel, Laurent Djakovitch

PII: S0926-860X(18)30203-5
DOI: https://doi.org/10.1016/j.apcata.2018.04.031
Reference: APCATA 16637

To appear in: *Applied Catalysis A: General*

Received date: 2-2-2018
Revised date: 18-4-2018
Accepted date: 23-4-2018

Please cite this article as: Rameau N, Russo B, Mangematin S, Pinel C, Djakovitch L, Stilbene synthesis through decarboxylative cross-coupling of substituted cinnamic acids with aryl halides, *Applied Catalysis A, General* (2010), https://doi.org/10.1016/j.apcata.2018.04.031

Stilbene synthesis through decarboxylative cross-coupling of substituted cinnamic acids with aryl halides

Nelly Rameau, Baptiste Russo, Stéphane Mangematin, Catherine Pinel, Laurent Djakovitch*

Univ Lyon, Université Claude Bernard Lyon 1, CNRS, IRCELYON, UMR 5256, 2 avenue Albert Einstein, F-69626 Villeurbanne, France.

** corresponding author: laurent.djakovitch@ircelyon.univ-lyon1.fr*

Graphical Abstract

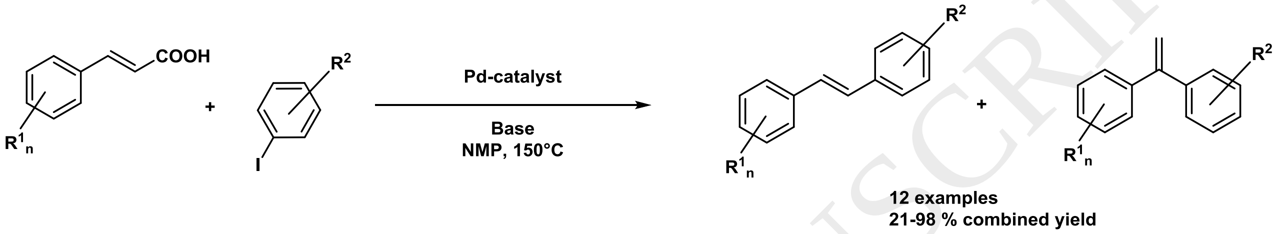

Highlights

- Pd-catalyzed decarboxylative cross-coupling of cinnamic acids and aryl iodide was studied.
- Both stilbenes and corresponding 1,1-biphenyl ethylene were produced at initial time.
- After optimization, homogeneous Pd(OAc)$_2$ gave up to 90% cross-coupling products combined yields with higher selectivity toward the stilbenes.
- Pd/C and home-made Pd/SiO$_2$ heterogeneous catalysts were also very effective in this reaction. Pd/SiO$_2$ was found more stable and reusable.

Abstract

The Pd-catalyzed decarboxylative cross-coupling reaction between cinnamic acid and aryl iodide derivatives was studied using both homogeneous and heterogeneous Pd-catalysts. It was demonstrated that simple Pd(OAc)$_2$ can catalyze this reaction with useful to high yields when engaging ferulic acid whatever the nature of the aryl iodide. However, limitations were found when varying the nature of the cinnamic acid derivatives mainly due to low decarboxylation process. This could be overcome in some cases by adding Cu(OH)$_2$/1,10-phenantroline as co-catalyst. In the presence of heterogeneous catalysts, the studies showed that both Pd/C and home-made Pd/SiO$_2$ catalysts afforded high product yields; however, while less active it was demonstrated that the Pd/SiO_2 catalyst could be reused over at least 4 cycles due to higher stability.

Keywords: decarboxylative coupling, stilbene synthesis, cinnamic acid, palladium, homogeneous catalysis, heterogeneous catalysis.

1. Introduction

Stilbenes are important class of compounds with usually C_{14} skeleton that found applications in agrochemical and pharmaceutical industries. For example, natural (poly)phenols stilbenes derivatives like Resveratrol, Pterostilbene or other Combretastatines A4 and analogues are recognized to have beneficial health effects such as cancer-preventive, protection against coronary heart disease, neuroprotective, anti-aging, anti-inflammatory [1, 2]. Other applications include liquid crystals for non-linear optic, polymer materials and lubricants. Additionally, stilbenes are also known as substructure of several macrocycles possessing interesting biological activity like the Marchantins and Riccardins [3-6].

All of these bioactive molecules (and substructures) are naturally available through extraction from higher plants families and fruits such as grapes and blackberries; however, in limited quantity. To face with such limitations and answer to the ever increasing demand, the synthesis of these compounds has attracted much attention in recent decades, and many reviews have been published on this subject [7-9]. Beside classical total syntheses mainly based on Wittig and Ullmann protocols generally illustrated through Resveratol [10-13], palladium catalyzed syntheses involving Heck [14-16], Suzuki [7, 17-19], Negishi [7, 20] or Stille [21, 22] cross-couplings were the object of intensive developments despite many negative environmental aspects like the use of toxic tin or boron compounds in Stille or Suzuki couplings, respectively (Figure 1).

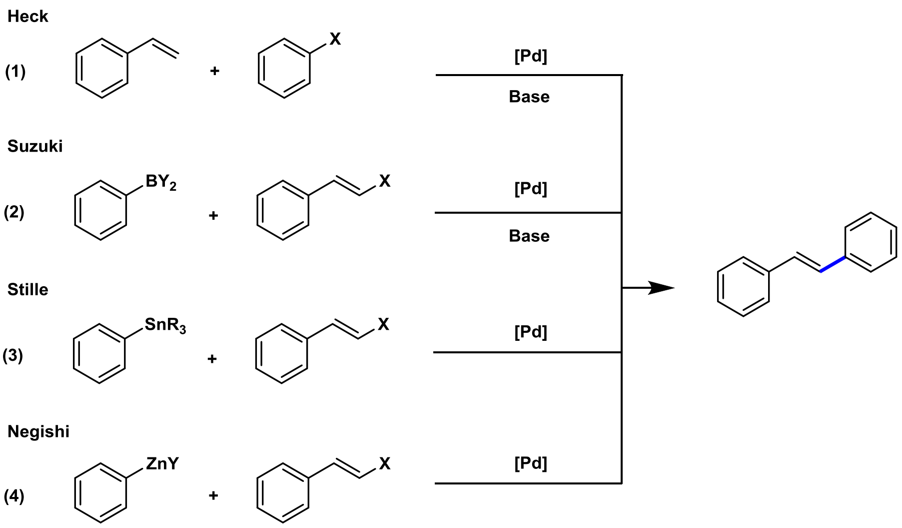

Figure 1: Common palladium catalyzed synthesis of stilbenes.

To face with these limitations, several authors developed the decarboxylative Heck coupling as an alternative and more elegant route for the synthesis of stilbene derivatives (Figure 2). This coupling allows benzoic acid derivatives to react with styrene derivatives in presence of palladium catalyst and a large excess of Ag_2CO_3. Although highly investigated, this route is today still limited to the use of *ortho*-substituted benzoic acids or α-heteroaromatic acids [23-29].

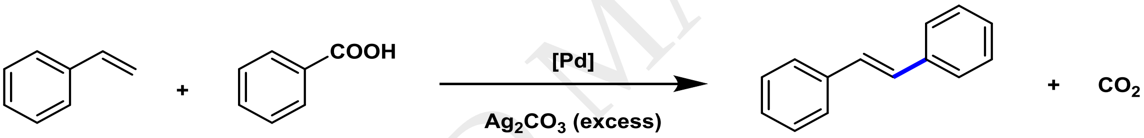

Figure 2: Decarboxylative Heck coupling toward stilbenes.

Alternative routes involve the decarboxylative coupling of commercially available cinnamic derivatives with aryl halides. The original methodology reported by Goossen et al. [30, 31] in the presence of palladium and copper catalysts, was further sporadically developed following this procedure [32-34] or using excess of silver carbonate in place of the copper catalyst [35, 36]. Recent progress involves a tandem Heck/Decarboxylation/Heck strategy to produce stilbene derivatives from aryl halides and acrylic acid [37]. In all these studies, the main limitation remains reaching efficient decarboxylation of the cinnamic derivatives that resulted in the use of additives, costly ligands or high temperatures.

Having in hands an efficient methodology to produce styrenes from cinnamic acids like the coumaric, ferulic or sinapic acids [38] that are readily available in large amount from renewables either as extracts from annual plants [39-42] or as by-product from lignin depolymerization [43], we were interested to revisit this methodology for producing stilbenes.

2. Experimental section

2.1 General informations: All commercial materials were used as received without further purification. NMP was purchased from Aldrich as anhydrous NMP in “sure-sealed bottle” and used without further treatment. Pd/C catalyst (E 105 CA/W 5%Pd_{wt}) was obtained from EVONIK. The Pd/SiO_2 catalyst (8.2 ± 0.1%wt Pd, particle size 5-11 nm) was prepared according the procedure previously reported by the wet impregnation method of agglomerated silica Aerosil 200 with $Pd(acac)_2$ in toluene followed by calcination under air flow [19, 44]. The palladium content determinations of the heterogeneous catalyst were performed by ICP-OES spectroscopy from a solution obtained by treatment of the catalysts with a mixture of HBF_4, HNO_3 and HCl in a Teflon reactor at 180 °C. Transmission electron microscopy (TEM) was carried out on a JEOL 2010 microscope with an instrumental magnification of 50 000x to 100 000x and an acceleration voltage of 200 kV. The point-to-point resolution of the microscope was 0.19 nm and the resolution between lines was 0.14 nm. The microscope is equipped with an EDX link ISIS analyzer from Oxford instruments. Energy-dispersive X-ray microanalysis (EDX) was conducted using a probe size of 25 nm to 100 nm to analyze grains of the phases. The powder samples were directly deposited on holey-carbon coated copper grid. X-ray powder diffraction (XRD) data were acquired on a Bruker D5005 diffractometer using Cu $K\alpha$ monochromatic radiation (λ = 1.054184 Å). GC analyses were performed on Agilent 4890 chromatograph equipped with a FID detector, a HP-5 column (cross-linked 5% phenyl-methylsiloxane, 30m x 0.25mm i.d. x 0.25µm film thickness) with nitrogen as carrier gas. Yields were determined by GC based on the relative area of GC-signals referred to an internal standard (dodecane) calibrated to the corresponding pure compounds. Purification of products was accomplished by flash chromatography at a pressure slightly greater than atmospheric pressure using silica (Merck Silica Gel 60, 230 - 400 mesh). Thin layer chromatography was performed on Fluka Silica Gel 60 F_{254}. Liquid ^1H NMR and ^{13}C NMR spectra were recorded in $(CD_3)_2CO$ at room temperature on a BRUKER AC-250 spectrometer. All chemical shifts were measured relative to residual ^1H or ^{13}C NMR resonances in the deuterated solvents: $(CD_3)_2CO$, δ 2.05 ppm for ^1H, 29.8 ppm for ^{13}C. The mass spectra were obtained on a Shimadzu GC-MS-QP2010S equipped with a AOC-20i+ autosampler and a Sulpelco SLB-5MS column (95% methylpolysiloxane + 5% phenylpolysiloxane, 30m x 0.25mm x 0.25µm) with He as carrier gas was used. The mass spectra were obtained on a Shimadzu GC-MS-QP2010S equipped with a AOC-20i+ autosampler and a Sulpelco SLB-5MS column (95% methylpolysiloxane + 5% phenylpolysiloxane, 30m x 0.25mm x 0.25µm) with He as carrier gas was used.

2.2 Typical procedure for the reaction of 1a with 2a

Ferulic acid (349 mg, 1.8 mmol), 4-iodoanisole (351 mg, 1.5mmol), $Pd(OAc)_2$ (22mg, 0.09 mmol), K_2CO_3 (414mg, 3 mmol) were added in a 25 mL round-bottom flask. The mixture of solids was deaerated by a series of vacuum/argon before adding under an argon flow anhydrous NMP (5mL). The reaction mixture was heated up to 80°C for 15h. After cooling to room temperature, the reaction mixture was diluted with ethyl acetate (20mL), HCl (10%) (5mL) and water (25mL). The aqueous layer was separated from the organic layer and extracted with ethyl acetate (3x20mL). The combined organic layers were washed with water and dried over $MgSO_4$ before being filtered and concentrated under reduced pressure. The residue was purified by flash column chromatography on silica gel using a mixture of ethyl acetate/petroleum ether as eluent to afford the stilbene **3a** as a white solid in 51% yield. ^{1}H NMR, ^{13}C NMR and MS (from GC-MS) are in full agreement with the literature (CAS 946613-59-8) [45, 46]. Side product **4a** was obtained as a yellow oil in 25% yield.

Data for **4a**: ^{1}H NMR (250 MHz, Acetone-D6), δ ppm: 7.66 (s, 1H), 7.34 – 7.22 (m, 2H), 6.97 – 6.86 (m, 3H), 6.85 – 6.72 (m, 2H), 5.27 (dd, *J* = 8.2, 1.5 Hz, 2H), 3.81 (s, 3H), 3.80 (s, 3H).^{13}C NMR (63 MHz, Acetone-d6) δ ppm: 160.45 (C), 150.56 (C), 148.01 (C), 147.50 (C), 134.98 (C), 134.31 (C), 130.17 (CH), 122.10 (CH), 115.47 (CH), 114.33 (CH), 112.48 (CH), 111.47 (CH_2), 56.26 (CH_3), 55.54 (CH_3). $C_{16}H_{16}O_3$ 256.11 g/mol, MS (EI): m/z (%) 256.00 (100.00), 240.95 (24.83), 225.95 (12.33), 224.95 (21.79), 153.00 (13.88), 152.00 (14.99), 141.05 (10.71)115.00 (11.51).

When, heterogeneous catalysts were used, the mass of catalyst was adapted regarding the Pd-loading on the material to reach the Pd-charge in the reaction (i.e. 0.06 equiv. [Pd]).

2.3 Typical procedure for monitoring the reaction of 1a with 2a:

Ferulic acid (349 mg, 1.8 mmol), 4-iodoanisole (351 mg, 1.5mmol), $Pd(OAc)_2$ (22mg, 0.09 mmol), K_2CO_3 (414mg, 3 mmol) were added in a 25 mL round-bottom flask. The mixture of solid was deaerated by a series of vacuum/argon before adding under an argon flow anhydrous NMP (5mL). The reaction mixture was heated up to 80°C for 15h. Once the reaction was started, time to time, aliquots (100µL) were removed from the mixture and analysed by GC or GC/MS after adding a calibrated amount of dodecane used as standard.

2.4 Typical procedure for leaching studies by hot-filtration for the heterogeneous catalysts:

Ferulic acid (349 mg, 1.8 mmol), 4-iodoanisole (351 mg, 1.5mmol), $Pd(OAc)_2$ (22mg, 0.09 mmol), K_2CO_3 (414mg, 3 mmol) were added in a 25 mL round-bottom flask. The mixture of solids was deaerated by a series of vacuum/argon before adding under an argon flow anhydrous NMP (5mL). The reactor was placed in a preheated oil bath at 80 °C. The reaction was conducted under vigorous stirring for 20 minutes of reaction. The supernatant solution was filtered through a cannula with a microglass Whatman filter (in order to remove all fine particles) and then treated for further 5 h under the standard reaction conditions. The reaction was monitored over the total period by GC and the results compared to a standard catalytic reaction.

2.5 Typical procedure for the recycling heterogeneous catalysts (Pd/C and PdO/SiO_2)

For recycling experiments the heterogeneous catalyst used in a first run was separated by centrifugation, washed with the 2 x 10 mL warmed anhydrous NMP and reused after drying at room temperature as described in the typical procedure for the reaction of **1a** with **2a**.

2.6 Data for isolated compounds 3 and 4.

Following isolated compounds gave spectroscopic data in agreement with the literature: **3b** (white solid, 83% yield) (CAS 102145-21-1) [47], **3c** (white solid, 65% yield) (CAS 1192280-85-5) [48], **3d** (white solid, 45% yield) (CAS 144336-66-3) [49, 50], **3e** (yellow solid, 22% yield) (CAS 124797-64-4) [51], **3g** (white solid, 5% yield) (CAS 1694-19-5) [52, 53], **3h** (white solid, 18% yield) (CAS 110993-22-1) [50], **3i** (white solid, 50% yield) (CAS 18951-44-5) [54, 55], **3k** (yellow solid, 6% yield) (CAS 15638-14-9) [56, 57], **3l** (yellow oil, 18% yield) (CAS 18513-95-6) [58], **3m** (white solid, 42% yield) (CAS 746636-48-6) [59], **4g** (white solid, 7% yield) (CAS 4333-75-9) [33], **4h** (yellow oil, 76% yield) (CAS 439659-96-8) [60], **4i** (yellow oil, 48% yield) (CAS 92549-05-8) [61], **4k** (yellow oil, 36% yield) (CAS 4356-69-8) [62, 63], **4l** (Yellow oil, 18% yield) (CAS 93652-35-8) [64].

3f: yellow solid, 50% yield. ^{1}H NMR (250 MHz, Acetone-D6), δ ppm: 7.89 – 7.83 (m, 2H), 7.51 – 7.44 (m, 2H), 7.10 – 7.03 (m, 2H), 7.00 – 6.90 (m, 2H), 6.84 (dt, *J* = 15.1, 1.0 Hz, 1H), 5.98 (s, 1H), 3.84 (s, 3H), 2.51 (s, 3H).^{13}C NMR (63 MHz, Acetone-d6) δ ppm: 197.03 (CO), 148.61 (C), 147.90 (C) , 137.73 (C) , 135.69 (C), 134.95 (CH) , 134.72 (CH) , 132.18 (C) , 128.41 (CH) ,127.26 (CH), 126.05 (CH) , 116.08 (CH) , 113.87 (CH), 56.10 (CH_3) , 26.75 (CH_3). $C_{16}H_{16}O_3$ 268.11 g/mol, MS (EI): m/z (%) 268.10 (100.00), 253.10 (55.53), 165.10 (26.71), 153.15 (10.46), 152.10 (14.79), 126.65 (18.15), 119.10 (10.29), 105.10 (11.08), 76.05 (15.83), 43.05 (61.24).

4b: yellow oil, 11% yield. ^{1}H NMR (250 MHz, Acetone-D6), δ ppm: 7.34 (td, *J* = 8.2, 1.8 Hz, 1H), 7.24 (dd, *J* = 7.7, 1.9 Hz, 1H), 6.99 (td, *J* = 7.4, 1.0 Hz, 1H), 6.92 (brd, *J* = 8.4 Hz, 1H), 6.90 (d, *J* = 1.9 Hz, 1H), 6.81 (d, *J* = 8.3 Hz, H), 6.74 (dd, *J* = 8.2, 1.9 Hz, 1H), 5.65 (d, *J* = 1.4 Hz, 1H), 5.30 (s, 1H), 5.22 (d, *J* = 1.4 Hz, 1H), 3.85 (s, 3H), 3.68 (s, 3H).^{13}C NMR (63 MHz, Acetone-d6) δ ppm: 157.04 (C), 146.60 (C), 146.14 (C), 145.17 (C), 133.49 (C), 131.23 (CH), 131.15 (C), 128.93 (CH), 120.55 (CH), 119.93 (CH), 113.83 (CH), 113.60 (CH_2), 111.14 (CH), 108.74 (CH), 55.86 (CH_3), 55.66 (CH_3). $C_{16}H_{16}O_3$ 256.11 g/mol, MS (EI): m/z (%) 256.10 (95.64), 241.05 (100.00), 213.05 (82.33), 181.05 (33.11), 153.10 (35.65), 152.10 (34.23), 115.05 (24.78), 76.00 (22.07).

4c: yellow oil, 11% yield. ^{1}H NMR (250 MHz, Acetone-D6), δ ppm: 7.26 (t, *J* = 7.5 Hz, 1H), 6.98-6.93 (m 1H), 6.93-6.88 (m, 4H), 6.86 (brd, *J* = 1.5 Hz, 1H), 5.69 (s, 1H), 5.40 (d, *J* = 1.4 Hz, 1H), 5.38 (d, *J* = 1.4 Hz, 1H), 3.85 (s, 3H), 3.81 (s, 3H).^{13}C NMR (63 MHz, Acetone-d6) δ ppm: 159.38 (C), 149.71 (C), 146.10 (C), 145.48 (C), 143.17 (C), 133.67 (C), 129.05 (CH), 121.64 (CH), 120.93 (CH), 114.00 (CH), 113.93 (CH), 113.23 (CH), 113.12 (CH_2), 110.72 (CH), 55.94 (CH_3), 55.24 (CH_3).

$C_{16}H_{16}O_3$ 256.11 g/mol, MS (EI): m/z (%) 256.15 (100.00), 195.10 (13.53), 181.10 (11.25), 153.10 (10.98), 152.10 (15.86), 115.10 (11.18).

4d: yellow oil, 19% yield. ^{1}H NMR (250 MHz, Acetone-D6), δ ppm: 6.95 (d, *J* = 8.4 Hz, 2H), 6.84 (d, *J* = 8.5 Hz, 1H), 6.79 (d, *J* = 8.4 Hz, 2H), 6.75 (dd, J = 8.4, 1.8 Hz, 1H), 6.70 (d, *J* = 1.8 Hz, 1H), 5.89 (brs, 2H), 5.59 (d, *J* = 1.1 Hz, 1H), 5.57 (d, *J* = 1.1 Hz, 1H), 3.92 (s, 3H).^{13}C NMR (63 MHz, Acetone-d6) δ ppm: 158.73 (C), 153.59 (C), 148.62 (C), 148.06 (C), 133.39 (C), 132.02 (CH), 131.67 (C), 124.73 (CH), 120.03 (CH_2), 116.31 (CH), 115.23 (CH), 114.87 (CH), 55.94 (CH_3). $C_{16}H_{16}O_3$ 242.09 g/mol, MS (EI): m/z (%) 243.10 (16.97), 242.05 (100.00), 227.05 (20.93), 211.05 (16.24), 199.05 (10.92), 181.05 (21.95), 153.05 (13.56), 152.10 (16.59), 115.05 (12.64), 91.00 (11.36), 76.05 (12.22), 55.00 (11.39).

4f: yellow solid, 7% yield. ^{1}H NMR (250 MHz, Acetone-D6), δ ppm: 7.84 (d, *J* = 8.6 Hz, 2H), 7.33 (d, *J* = 8.4 Hz, 2H), 6.80 (d, *J* = 8.4 Hz, 1H), 6.79 (d, *J* = 2.0 Hz, 1H), 6.65 (dd, *J* = 8.5, 1.9 Hz, 1H), 5.93 (s, 1H), 5.62 (s, 2H), 3.91 (s, 3H), 2.54 (s, 3H).^{13}C NMR (63 MHz, Acetone-d6) δ ppm: 197.36 (CO), 153.53 (C), 148.59 (C), 148.08 (C), 141.87 (C), 137.39 (C), 130.76 (CH), 128.49 (CH), 124.71 (CH), 120.05 (CH_2), 116.29 (CH), 114.89 (CH), 55.99 (CH_3), 26.40 (CH_3). $C_{16}H_{16}O_3$ 268.11 g/mol, MS (EI): m/z (%) 269.20 (18.27), 268.25 (100.00), 254.20 (12.81), 253.20 (71.99), 165.15 (29.88), 153.20 (14.01), 152.15 (18.90), 126.65 (18.98), 105.10 (11.79), 76.10 (19.36), 43.10 (84.03).

4m: yellow oil, 8% yield. ^{1}H NMR (250 MHz, Acetone-D6), δ ppm: 7.12 (d, *J* = 8.5 Hz, 2H), 7.04 (d, *J* = 8.5 Hz, 2H), 6.48 (s, 2H), 5.98 (s, 1H), 5.56 (s, 1H), 5.59 (s, 1H), 3.92 (s, 6H), 3.78 (s, 3H). ^{13}C NMR (63 MHz, Acetone-d6) δ ppm: 153.65 (C), 147.79 (C), 139.34 (C), 134.21 (C), 132.29 (C), 131.96 (CH), 119.62 (CH_2), 112.89 (CH), 108.79 (CH), 56.39 (CH_3), 55.31 (CH_3). $C_{16}H_{16}O_3$ 286.12 g/mol, MS (EI): m/z (%) 287.05 (19.11), 286.05 (100.00), 271.05 (9.34), 256.00 (6.51), 255.05 (10.49), 240.05 (6.14), 239.00 (7.64), 225.00 (5.15), 211.00 (13.42), 152.10 (6.18), 140.05 (5.49), 139.05 (8.83), 128.05 (10.65), 127.05 (8.06), 115.05 (6.43).

3. Results and discussion

In order to develop further the synthesis of functional stilbenes from cinnamic acid derivatives, we explored the decarboxylative cross-coupling between ferulic acid **1a** that is readily available in large amount from market and 4-iodoanisole **2a** (Scheme 1), focusing on the formation of stilbene **3a**. 1,1-biphenyl ethylene **4a**, can be observed as a co-product of the reaction [33].

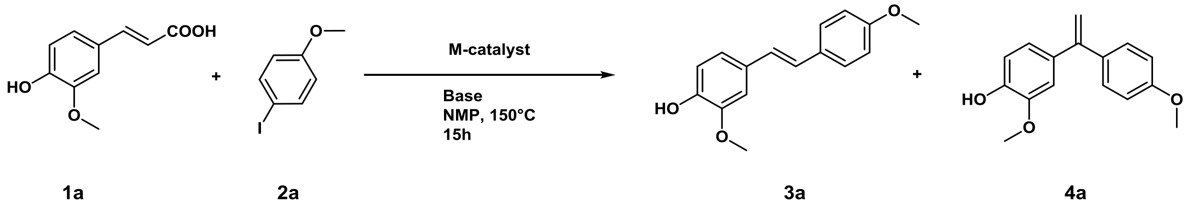

Scheme 1 : Decarboxylative cross-coupling of ferulic acid and 4-iodoanisole as a benchmark reaction.

Initially, the reaction was carried out using the optimized conditions achieved for the decarboxylation of cinnamic acids, i.e.: $Cu(OH)_2$ (0.06 equiv.) in presence of phenanthroline (0.12 equiv.) and K_2CO_3 (2 equiv.) in NMP (5mL) at 150°C for 15h [38]. Under these conditions, neither **3a**, nor **4a** were observed (Table 1, entry 1). The only observed products corresponded to those of the proto-decarboxylation of the ferulic acid and dehalogenation of 4-iodoanisole. Thus, copper used alone as catalyst was not efficient to perform such decarboxylative cross-coupling. Following the procedures described previously by Goossen et *al.* on decarboxylative cross-coupling of benzoic acid with arylhalides [30, 31], a palladium source was added in catalytic amount to the reaction mixture. Thus, adding 0.06 equiv. $Pd(OAc)_2$ afforded the desire products in 84% yield with a **3a**:**4a** ratio of 70:30 (Table 1, entry 2). As expected from reported mechanisms, in absence of base (K_2CO_3) the combined yields of **3a+4a** dropped to 4% (Table 1, entry 3) whereas in absence of copper source the combined yields remained as high as 78% without noticeable modifications in the **3a**:**4a** ratio (Table 1, entry 4). However, it was noticed that while phenanthroline ligand was believed to stabilize copper co-catalyst, in its absence the combined product yields decreased to 63% outlining its role as Pd-species stabilizer by limiting probably Pd-black formation (Table 1, entry 5).

To conclude on these preliminary studies, the high yield (78%) obtained for **3a**/**4a** using $Pd(OAc)_2$/phenanthroline/K_2CO_3 catalytic system encouraged us to optimise further this procedure.

Table 1: Preliminary studies on the decarboxylative cross-coupling reaction of ferulic acid with 4-iodoanisole.[a]

Entry	Copper	Palladium	Ligand	Base	Conv. (%)[b]	Yield (3a+4a) (%)[b]	Ratio (3a:4a)
1	$Cu(OH)_2$	-----	Yes	K_2CO_3	72	0	-----
2	$Cu(OH)_2$	$Pd(OAc)_2$	Yes	K_2CO_3	100	84	70:30
3	$Cu(OH)_2$	$Pd(OAc)_2$	Yes	-----	86	4	70:30
4	-----	$Pd(OAc)_2$	Yes	K_2CO_3	100	78	70:30
5	-----	$Pd(OAc)_2$	No	K_2CO_3	99	63	74:26

[a] Reaction condition: ferulic acid (0.8 mmol), 4-iodoanisole (0.5 mmol), $Cu(OH)_2$ (0.06 equiv.), $Pd(OAc)_2$ (0.06 equiv.), phenanthroline (0.12 equiv.), Base (2 equiv.), NMP (5mL), 150°C, 15h. [b] Conversions and yields determined by GC.

As a first optimization step, we evaluated several Pd-sources including several commercially available palladium salts and complexes (Table 2, entries 1-6) that were selected according our previous report on decarboxylative heterocoupling coupling of substituted benzoic acids to biaryls [65], other parameters like solvent and base, being kept. Whatever the PdX_2 salt (X=OAc, Cl, Br, I) used as catalyst precursor, little differences were observed, all leading almost to the same 76-82% combined yields in expected products with a **3a**:**4a** ratio of *ca.* 70:30. Noticeably, the Beller-Herrmann's palladacycle gave higher selectivity in **3a** with a **3a:4a** ratio of 80:20 (Table 2, entry 6). The lack of influence of the palladium source could indicate that, in all cases similar active Pd^0-species are generated from these precursors, more probably in equilibrium with small Pd-particles or Pd-colloids serving as Pd-storage [66] (see propose mechanisms, Figure 11).

Since little influence of the palladium source was observed, we decided to proceed using the $Pd(OAc)_2$ as catalyst in order to enhance further the yield in stilbene **3a**.

Table 2: Influence of the nature of the palladium catalysts on the decarboxylative cross-coupling reaction of ferulic acid with 4-iodoanisole.[a]

Entry	[Pd]	Conv. (%)[b]	Yield (3a+4a) (%)[b]	Ratio (3a:4a)
1	$Pd(OAc)_2$	97	78	68:32
2	$PdCl_2$	98	76	67:31
3	$PdBr_2$	100	76	70:30
4	PdI_2	95	82	68:32
5	$Pd_2(dba)_3$	97	77	71:29
6	Palladacycle[c]	88	82	80:20

[a] Reaction condition: ferulic acid (1.8 mmol), 4-iodoanisole (1.5 mmol), [Pd] (0.06 equiv.), K_2CO_3 (2 equiv.), NMP (5mL), 80°C, 15h. [b] Conversions and yields determined by GC. [c] NaOAc was used as the base and reaction were performed at 150°C. [d] after 6h reaction time at 130°C.

Several reaction parameters were evaluated in order to optimize the yields in stilbene/biphenyl **3a+4a**, including the temperature (Table 3), the solvent (Table 4) and the nature of the base (Table 5). Varying the reaction temperature from 40°C to 150°C, allowed to improve the conversion of **1a** after 15h reaction time from 47% to nearly quantitative that is reached above 80°C. At the same time the combined yields of **3a+4a** increased up to 78% at 80°C before decreasing (Table 2, entry 3); this reaction temperature afforded also the highest selectivity (80%) in desired products. Little influence of the reaction temperature on the **3a:4a** ratio was observed, the highest ratio in **3a** being obtained at 150°C. This result can be explained by considering the formation of both isomers that includes two-reaction steps, a decarboxylation and a CC-coupling reactions that proceed more probably with different reaction rates. According to scheme 2, **3a** can be obtained via two pathways: route A involves firstly a protodecarboxylation producing the 4-vinylguaiacol **7a** that undergoes a Heck coupling reaction to give the expected stilbene **3a**. Alternatively, **3a** can be obtained by route B that involves a CC-coupling reaction to deliver the intermediate stilbene **5a** that gives **3a** upon protodecarboxylation. It is believed that **4a** is almost exclusively formed via route C through the intermediate **6a**. From our previous report [38], the protodecarboxylation is relatively slow at low temperature; therefore, route B and C will be favored producing slightly higher **3a:4a** ratios. On the contrary at, and above, 110°C, the protodecarboxylation of **1a** is efficient making route A predominant for enriching the reaction mixture in **3a**.

Table 3: Influence of the temperature on the decarboxylative cross-coupling reaction of ferulic acid and 4-iodoanisole.[a]

Entry	Temperature (°C)	Conv. (%)[b]	Yield (3a+4a) (%)[b]	Ratio (3a:4a)	Selectivity[c]
1	40	47	7	64:36	15
2	60	69	48	70:30	70
3	80	97	78	68:32	80
4	110	98	77	70:30	78
5	150	99	63	74:26	64

[a] Reaction condition: ferulic acid (0.8 mmol), 4-iodoanisole (0.5 mmol), $Pd(OAc)_2$ (0.06 equiv.), K_2CO_3 (2 equiv.) NMP (5mL), 15h. [b] Conversions and yields determined by GC.[c] Selectivity = Yield (**3a+4a**)/Conversion.

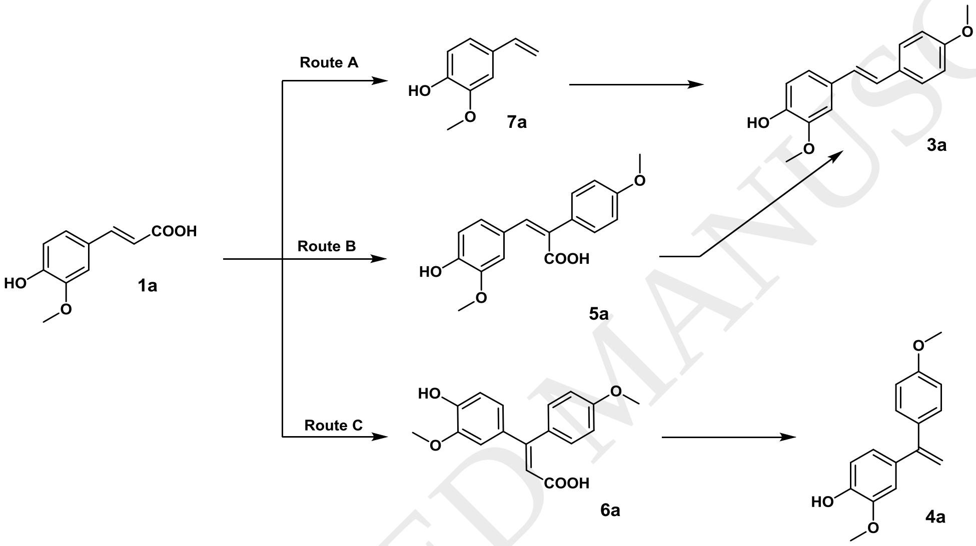

Scheme 2: Pathways delivering **3a** or **4a** in the decarboxylative cross-coupling of ferulic acid and 4-iodoanisole.

Then, with the aim of improving further the yields in **3a+4a** and possibly **3a** selectivity, other reaction parameters (nature of solvent, nature and loading of the base, loading of palladium salt), selected from our own expertise and review of current literature [67-70], were evaluated at 80°C using $Pd(OAc)_2$ as catalyst precursor (Tables 4-6). Except in 1,3-propanediol and PEG-2000 (Table 4, entry 4) for which the yields in excepted coupling products **3a+4a** were low (35% with a ratio **3a:4a** of 78:22) due to the protic nature of these solvents, good results were achieved in more classical NMP, DMA and DMF with combined **3a+4a** yields of 78%, 74% and 69% respectively (Table 4, entries 1-3). In these solvents, the ratio **3a:4a** was close to 70:30. Therefore, NMP was used in following optimisations. Regarding bases (Table 5), clearly the best result was obtained using K_2CO_3 (Table 5, entry 1); further optimisation demonstrated that using 0.5-1.5 equiv. provided further yield enhancements up to 88% with 1 equiv. K_2CO_3 (Figure 3) with a slight increase of the selectivity toward **3a**. Under these conditions (ferulic acid (0.8 mmol), 4-iodoanisole (0.5 mmol), $Pd(OAc)_2$ (x equiv.), K_2CO_3 (1 equiv.) NMP (5 mL), 80°C, 15h) the loading of palladium catalyst was optimized; using 0.06 equiv. of $Pd(OAc)_2$ provided the highest yield (88%) in **3a+4a** with a **3a:4a** ratio of 75:25 (Table 6). Following the evolution of the reaction mixture *versus* the time demonstrated that both products, **3a** and **4a**, were produced simultaneously with a constant selectivity close to **3a:4a** *ca.* 70:30. While the initial activity was over A_i=6.0 $mol_{(\mathbf{3a+4a})}/mol_{Pd}/h$, it decreased after 1 hour to stabilize after 2 hours to A_{des}=0.7 $mol_{(\mathbf{3a+4a})}/mol_{Pd}/h$ probably due to catalyst deactivation as observed from Pd-black formation. Upon the time, side products, mainly due to the protodecarboxylation, were observed (Figure 4).

Table 4: Influence of the nature of the solvent on the decarboxylative cross-coupling reaction of ferulic acid and 4-iodoanisole.[a]

Entry	Solvent	Conv. (%)[b]	Yield (3a+4a) (%)[b]	Ratio (3a:4a)
1	NMP	97	78	68:32
2	DMF	91	69	64:36
3	DMA	96	74	68:32
4	Propanediol	96	35	78:22
5	PEG 2000	98	35	79:21

[a] Reaction condition: ferulic acid (0.8 mmol), 4-iodoanisole (0.5 mmol), $Pd(OAc)_2$ (0.06 equiv.), K_2CO_3 (2 equiv.) solvent (5mL), 80°C, 15h. [b] Conversions and yields determined by GC.

Table 5: Influence of the nature of the base on the decarboxylative cross-coupling reaction of ferulic acid and 4-iodoanisole.[a]

Entry	Base	Conv. (%)[b]	Yield (3a+4a) (%)[b]	Ratio (3a:4a)
1	K_2CO_3	97	78	68:32
2	NaOAc	75	61	73:27
3	NaOH	75	38	70:30
4	Na_2CO_3	58	38	66:34

[a] Reaction condition: ferulic acid (0.8 mmol), 4-iodoanisole (0.5 mmol), $Pd(OAc)_2$ (0.06 equiv.), Base (2 equiv.), NMP (5mL), 80°C, 15h. [b] Conversions and yields determined by GC.

Table 6: Influence of palladium loading on the decarboxylative cross-coupling reaction of ferulic acid and 4-iodoanisole.[a]

Entry	$Pd(OAc)_2$	Conv. (%)	Yield (3a+4a)	Ratio (3a:4a)
1	0	72	0	-
2	0.01	88	77	82:18
3	0.02	87	81	81:19
4	0.04	93	86	78:22
5	0.06	99	88	75:25
6	0.08	95	89	73:27
7	0.1	96	85	71:29

[a] Reaction condition: ferulic acid (0.8 mmol), 4-iodoanisole (0.5 mmol), Pd(OAc)$_2$, K_2CO_3 (1 equiv.), NMP (5mL), 80°C, 15h. [b] Conversion and yield determined by GC.

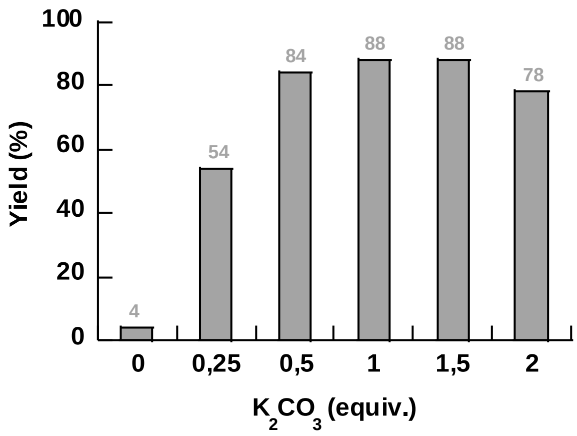

Figure 3: Influence of base loading on the decarboxylative cross-coupling reaction of ferulic acid and 4-iodoanisole. Reaction condition: ferulic acid (0.8 mmol), 4-iodoanisole (0.5 mmol), Pd(OAc)$_2$ (0.06 equiv.), K_2CO_3, NMP (5mL), 80°C, 15h. Conversion and yield determined by GC.

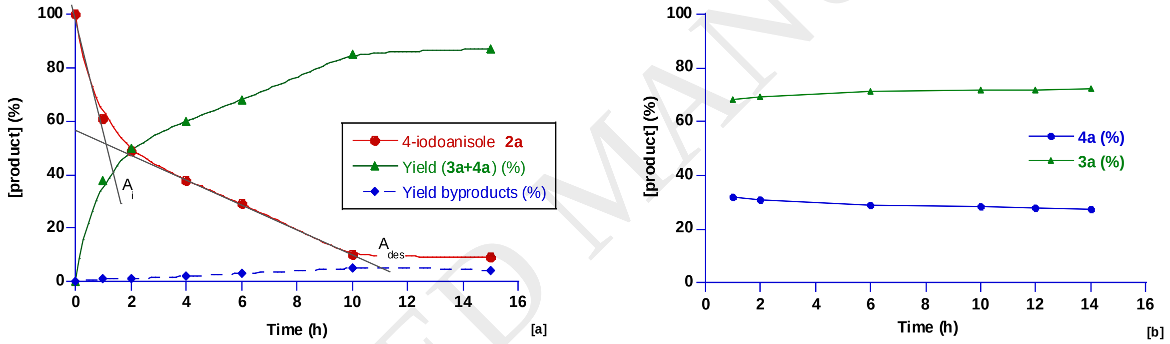

Figure 4: Reaction monitoring over the time in the decarboxylative cross-coupling reaction of ferulic acid and 4-iodoanisole at 80 °C. [a] Conversion of **2a** and Yield of **[3a+4a]** versus the time; [b] **3a/4a** selectivity versus the time. Reaction conditions: ferulic acid (0.8 mmol), 4-iodoanisole (0.5 mmol), Pd(OAc)$_2$ (0.06 equiv.), K_2CO_3 (1 equiv.), NMP (5mL). Conversion and yield determined by GC.

With these conditions in hand (cinnamic acid (0.8 mmol), aryl iodide (0.5 mmol), Pd(OAc)$_2$ (0.06 equiv.), K_2CO_3 (1 equiv.) NMP (5 mL), 110°C, 15 h), we then evaluated the scope and limitations of the reaction using either various aryl iodides or various cinnamic derivatives (Tables 7-8). Exploring the different isomers of iodoanisole (i.e.: *o*-, *m*- and *p*-iodoanisole), the results demonstrated that the reactivity follows the general rule, i.e.; ortho >para > meta giving 94%, 78% and 62% **3+4** combined yields, respectively whereas the **3:4** ratio seems to be influenced by the position of the substituent, the *ortho* derivative leading to the lowest **3** selectivity (Table 7, entries 1-3). On the other hand, the electronic nature of the substituent on the aryl iodide influenced more strongly the outcome of the reactions. On the contrary to what is generally observed in classical Heck (and associated) coupling reactions, aryl iodides substituted by electron donating groups (OMe and OH) provided higher **3+4** yields (resp. 78% and 64%, respectively Table 7 entries 3 and 4) than those bearing electron withdrawing groups (NO_2, CH_3CO) that gave 22% and 57% **3+4** yields, respectively (Table 7, entries 5 and 6) together with high level of nitrobenzene and acetophenone issued from dehalogenation reaction. This can be related to competitive dehalogenation and cross-coupling reactions both being catalyzed by Pd-species. Since the rate of the cross-coupling reaction involving decarboxylative step was relatively low for these highly reactive substrates, then dehalogenation was predominant.

Table 7: Influence of the nature of the aryl iodide on its decarboxylative cross-coupling with the ferulic acid.[a]

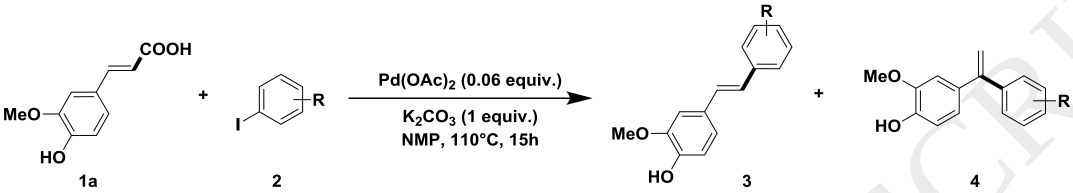

Entry	ArI	Yield (3+4) (%)[b]	Ratio (3:4)
1	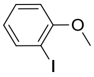 [2b]	94	$88_{[3b]}$:$12_{[4b]}$
2	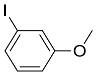 [2c]	62	$87_{[3c]}$:$13_{[4c]}$
3	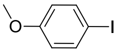 [2a]	78	$67_{[3a]}$:$33_{[4a]}$
4	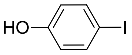 [2d]	64	$70_{[3d]}$:$30_{[4d]}$
5	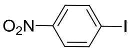 [2e]	22	$100_{[3e]}$:0
6	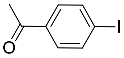 [2f]	57	$87_{[3f]}$:$13_{[4f]}$

[a] Reaction conditions: ferulic acid (1.8 mmol), aryl iodide (1.5 mmol), $Pd(OAc)_2$ (0.06 equiv.), K_2CO_3 (1 equiv.), NMP (7mL), 110°C, 15 h. [b] Yields determined by GC.

Next, eight potentially biosourced cinnamic acid derivatives were evaluated for coupling with p-iodoanisole. They differ by the number and the nature (OH / OMe) of the substituents on the aromatic ring. Using the reaction conditions reported above, ferrulic acid **1a**, *p*-hydroxycinnamic acid **1i**, and *m*-hydroxycinnamic acid **1h** gave, moderate to low 78%, 75% and 24% **3+4** yields, resp., (Table 8, entries 1, 3 and 4) while no reaction was observed with the other substituted cinnamic acid derivatives despite higher temperature (i.e. 130°C). Based on previous studies [38, 65], we assumed that the lack of reactivity was linked to the difficulty to decarboxylate these substrates. This encouraged us to add to the reaction mixture [$Cu(OH)_2$/1.10-phenanthroline] as co-catalyst ($Cu(OH)_2$ (0.06 equiv.), 1,10-phenanthroline (0.12 equiv.)) known to catalyze the decarboxylation reaction. Under these modified conditions, the yields in cross-coupling products implying **1h** and **1i** were improved to 94% and 98%, respectively. Except caffeic acid **1j** that did not react and was recovered at the end of the reaction even at 180°C (Table 8, entry 5), all other substrates led to cross-coupling reactions with 4-idoanisole **2a** giving low to moderate yields (Table 8, entries 2, 6-8). In these examples, the main difficulty remained the low efficiency of the decarboxylation of the cinnamic acids to afford the expected coupling compounds **3+4** in high yields. Working at higher temperature did not generally improve the situation since the competitive dehalogenation of 4-iodoanisdole was also strongly accelerated.

Table 8: Influence of the nature of the cinnamic acid on its decarboxylative cross-coupling with the 4-iodoanisole.[a]

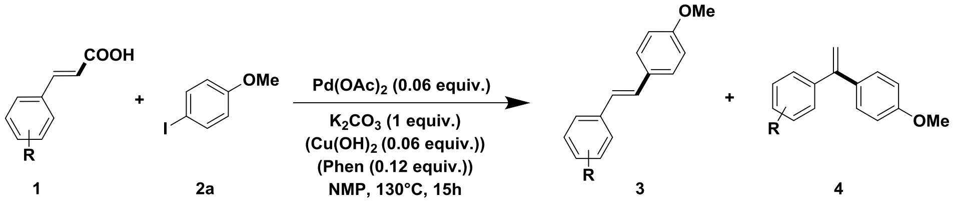

Entry	Cinnamic acid	Yield (3+4) (%)[b]		Ratio (3:4)	
		A	B	A	B
1	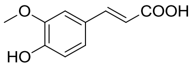 [1a]	78	80	$70_{[3a]}:30_{[4a]}$	$73_{[3a]}:27_{[4a]}$
2	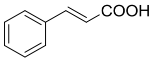 [1g]	-	12	-	$37_{[3g]}:63_{[4g]}$
3	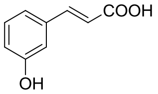 [1h]	24	94	$36_{[3h]}:64_{[4h]}$	$19_{[3h]}:81_{[4h]}$
4	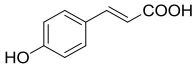 [1i]	75	98	$45_{[3i]}:55_{[4i]}$	$51_{[3i]}:49_{[4i]}$
5	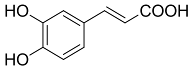 [1j]	-	0	-	-
6	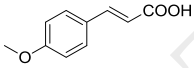 [1k]	-	42	-	$14_{[3k]}:86_{[4k]}$
7	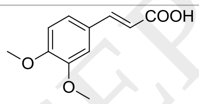 [1l]	-	21	-	$15_{[3l]}:85_{[4l]}$
8	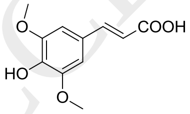 [1m]	-	50	-	$87_{[3m]}:13_{[4m]}$

[a] Reaction condition: Conditions A : cinnamic acid (1.8 mmol), aryl iodide (1.5 mmol), $Pd(OAc)_2$ (0.06 equiv.), K_2CO_3 (1 equiv.), NMP (7mL), 130°C, 15 h. Conditions B : cinnamic acid (1.8 mmol), aryl iodide (1.5 mmol), $Pd(OAc)_2$ (0.06 equiv.), $Cu(OH)_2$ (0.06 equiv.), 1,10-phenantroline (0.12 equiv.), K_2CO_3 (1 equiv.), NMP (7mL), 130°C, 15 h. [b] Yields determined by GC.

In addition, we have performed the coupling reaction in the presence of heterogeneous catalysts. Two types of supported palladium catalysts were evaluated and their characterization is reported.

The Pd/C catalyst type E105 CA/W (3.5%wt Pd determined by AAS) was provided by Evonik and characterized by TEM and XRD. TEM (Figure 5a) showed a heterogeneous Pd repartition with an average Pd particle size of 4.7 nm (standard deviation: 3.3 nm). XRD exhibited few crystallites attributed mainly to PdO species with characteristic 2θ at 34.03° (PdO (101)) with an average particle size of 3-8 nm calculated according to Scherrer equation (Figure 6a). These value are slightly higher than previous reports on this catalyst (average Pd particle size of 2.6 nm determined by chemisorption) [71, 72]. Pd at oxidation state Pd^0 was also observed with a characteristic 2θ at 43.15° (Pd (111)), while unexpected given the preparation methodology of this Pearlman type catalyst, that was probably due to partial catalyst reduction during experiment. These data are in agreement with those obtained from XPS analysis that exhibit peaks at 337.4 eV (70%) and 338.6 eV (8.9%) attributed to Pd^{2+}-species, together with signals at 335.3 eV (14.4%) attributed to Pd^0-species and 336.1 eV (6.7%) that could be due to either Pd^0 or Pd^{1+}-species according a report from Zharmagambetova et al. [73] (Figure 7).

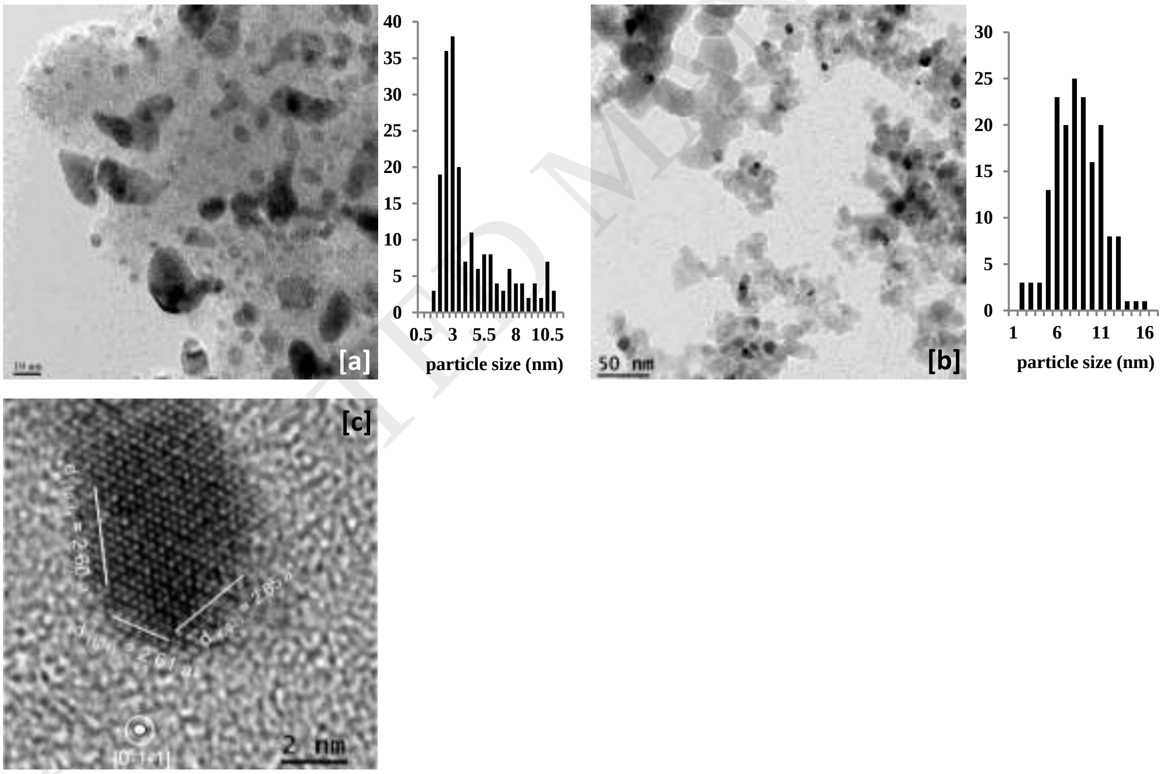

Figure 5: TEM of [a] the fresh Pd/C catalyst with corresponding histogram of Pd particle size distributions (N = 200) and [b] and [c] fresh Pd/SiO_2 catalyst at two magnifications and corresponding histogram of PdO particle size distribution (N = 200).

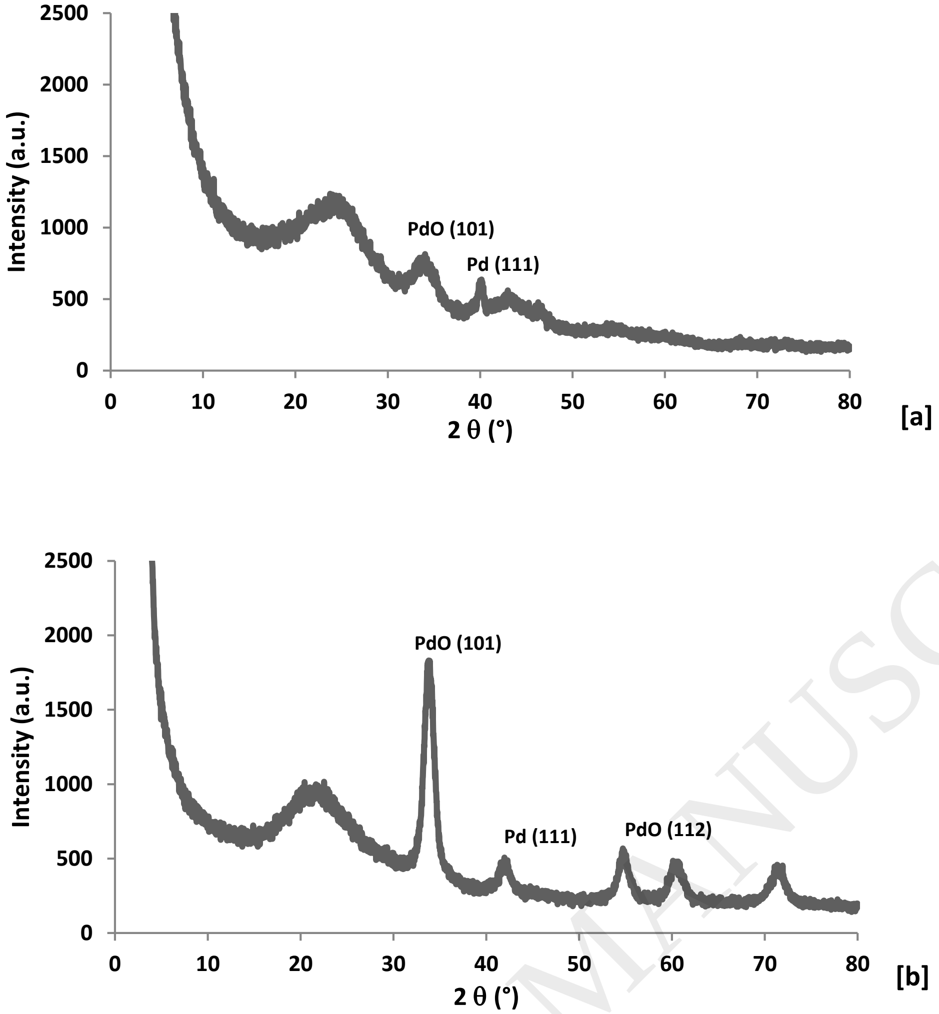

Figure 6: XRD of the fresh Pd/C [a]and Pd/SiO_2 [b] catalysts.

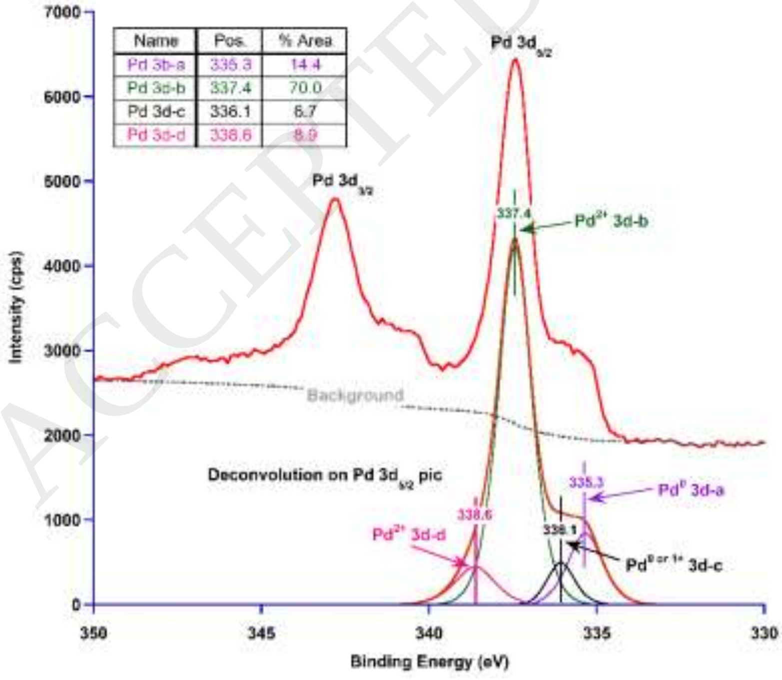

Figure 7: XPS of the fresh Pd/C catalyst. Deconvolution of the $Pd3d_{5/2}$ exhibits value at 338.6eV (9%), 337.4eV (70%), 336.1eV (7%) and 335.3eV (14%). The latter is probably related to partial reduction under electron beam.

Pd/SiO_2 (Pd/SiO_2 8.9%wt Pd) was prepared according to procedure reported in the literature by the wet impregnation method of agglomerated silica Aerosil 200 with $Pd(acac)_2$ in toluene followed by calcination under air flow[19, 44] and was fully characterized. XRD analysis indicated that immobilized palladium phase corresponds mainly to crystalline palladium oxide with characteristic diffraction peaks of 2θ at 33.87° (PdO (101)) and 54.70° (PdO (112)) with an average particle size of 6-10 nm calculated according to Scherrer equation (Figure 6b)[74]. A low intensity signal of 2θ at 40.12° (Pd (111)) indicated the presence of reduced palladium. However, it cannot be excluded that this reduction occurs during XRD measurements that is supported by the absence of Pd^0 particles in TEM and agree previous XPS characterizations [44]. TEM of the fresh catalyst clearly showed particles with an average size of 8 nm with standard deviation of 1.8 nm (Figure 5b and 5c) which diffractogram exhibited lattice fringes at 2.60 Å, 2.61 Å and 2.65 Å corresponding respectively to (10-1), (101) and (002) crystallographic planes of PdO.

Both heterogeneous catalysts were evaluated for the decarboxylative cross-coupling reaction of ferulic acid with 4-iodoanisole. Due to lower activity of these heterogeneous catalysts compared to the homogeneous ones, the reactions were carried out at 130°C vs 80°C. Regular samplings allowed to establish the profile of the decarboxylative cross-coupling reaction of ferulic acid with 4-iodoanisole (conditions: ferulic acid (1.8 mmol), 4-iodoanisole (1.5 mmol), [Pd] (3mol%), K_2CO_3 (2 equiv.), NMP (5mL), 130°C, 6 h) (Figure 8). Using Pd/SiO_2 catalyst, as expected a short induction period of *ca.* 5 min, related to surface reaction occurring mainly at corner and edge atoms of the supported large PdO-particles before delivering dissolved Pd-species in reaction media, was observed before detecting products. Then the catalyst was active with an A_{max}= 19 $mol_{(\mathbf{3a+4a})}/mol_{Pd}/h$ (i.e. corresponding to the highest rate) affording finally 82% **3a+4b** yield after 3 h. Like with homogeneous $Pd(OAc)_2$ catalyst both coupling products **3a** and **4b** were produced simultaneously, and the **3a:4a** ratio stabilized after *ca.* 1 h to 85:25. With Pd/C catalyst, no induction period could be clearly observed and the catalyst presented a higher activity of A_{max}= 33 $mol_{(\mathbf{3a+4a})}/mol_{Pd}/h$ before slowly deactivating after 1 hour. The absence of induction period using the Pd/C catalyst can be directly related to the average particle size of the Pd-species onto the carbon support that was shown to be initially smaller (i.e. 4.7 nm for Pd/C *versus* 8nm for Pd/SiO_2). Finally, 98% yield in **3a+4a** was obtained after 6 hours with a **3a:4a** ratio of *ca.* 75:25 (stabilized after 1 hour). For both catalysts, while more pronounced with Pd/C, 4-iodoanicole consumption was more rapid than product **3a+4a** formation. This can be related to a two steps formation of **3a**/**4a** that involves two consecutive reactions with different reaction rates. According to scheme 2, we assume that **3a**/**4a** were mainly obtained through route B and C, i.e. as a sequence involving initial oxidative addition of the aryliodide on Pd(0)-species followed by the cross-coupling reaction before the decarboxylative step that deliver the products. The first steps are initiated by Pd(0)-species whereas the last step is mainly catalysed by Pd(II)-species in our case. This was supported by detection of intermediates **5a** and **6a**; however in low amount.

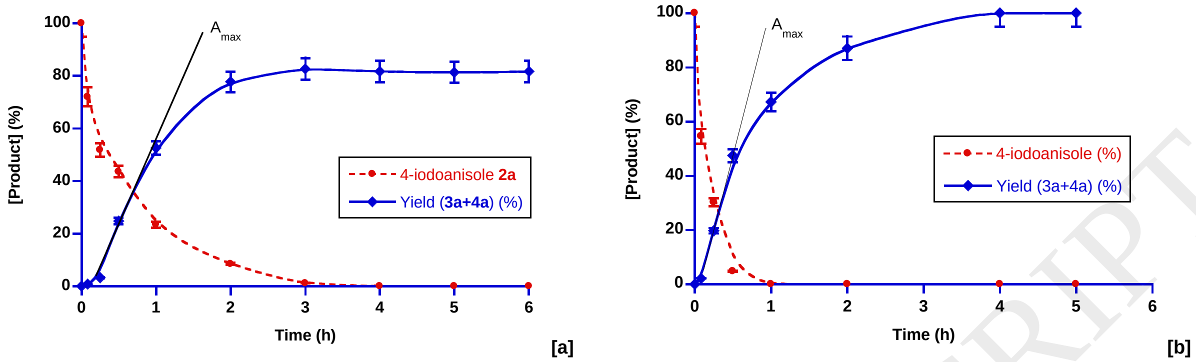

Figure 8: Conversions and Yields versus the time for the decarboxylative coupling reaction of ferulic acid with 4-iodonaisole. a) Pd/SiO_2, b) Pd/C. Reaction conditions: ferulic acid (1.75 mmol), aryl iodide (1.5 mmol), [Pd] (3mol%), K_2CO_3 (2 equiv.), NMP (5mL), 130°C, 6 h. Yields and conversions determined by GC.

In order to get better insight regarding the real activity of these two heterogeneous catalyst, hot-filtration test [75, 76] was performed. Thus, a catalytic run was started as for a standard reaction, and after 15 min of reaction, the hot reaction mixture was filtered through a celite pad to afford a clear filtrate that was then treated as a standard catalytic run and its evolution was followed by GC. The results were compared to that of a standard catalytic run (Figure 9). Initially, the experiment was conducted using the PdO/SiO_2 catalyst. After hot-filtration, the results showed only little progression of the combined **3a+4a** yield from 8 to 10%. However, we observed that the base used, K_2CO_3, was not fully soluble in the reaction media; therefore, another experiment was conducted by adding to the clear filtrate a new charge of K_2CO_3 (2 equiv.). In that case, the yield of **3a+4a** progressed from 8% just after the end of the filtration procedure to 26% after 4 hours reaction (Figure 6a). The experiment conducted using Pd/C catalyst (after addition of a new charge of base) indicated more clearly an increase of the combined yield after hot-filtration as it progressed from 33% after hot-filtration to 84% after 4 hours (Figure 9b). These results indicated that dissolved palladium released from the support *via* the oxidative addition of the aryliodide according the dissolution/redeposition mechanism [15, 77-79], contributed to the decarboxylative cross-coupling reaction. In both cases, deactivation of the dissolved Pd-species in the clear filtrate was observed.

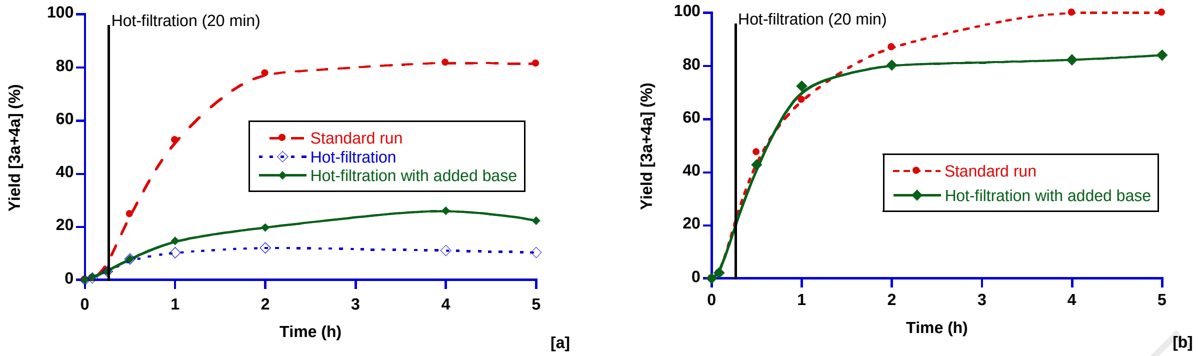

Figure 9: Residual catalytic activity after Hot-filtration ◆ after 15 min reaction versus standard catalytic ■ run. [a] Pd/SiO_2 and [b] Pd/C. Reaction conditions: ferulic acid (1.75 mmol), aryl iodide (1.5 mmol), [Pd] (3mol%), K_2CO_3 (2 equiv.), NMP (5mL), 130°C, 6 h. Yields and conversions determined by GC.

Further information was provided by determining the level of Pd lixiviation in each case at 20 minutes of reaction (Table 9). Data indicated that the level of Pd leaching for the Pd/C catalyst was much higher (2.7%) than that of Pd/SiO_2 (0.5%) that reflect, as expected from literature [80], the large differences in term of particle size. According that origin of leaching, and related catalytic activity, take place on low-coordinate Pd-atoms that are found mainly at the edge and corner sites of Pd-particles, this observation is then directly supported by TEM characterizations of prepared catalysts. Considering that only dissolved species were responsible for observed product formation, the Pd/SiO_2 and Pd/C catalysts reached activity of $A_{max\text{-}cor}$= 3840 and 1260 $mol_{(\mathbf{3a+4a})}/mol_{leached\text{-}Pd}/h$, respectively. However, this simple calculation, while informative, did not reflect the rate of deactivation of the dissolved Pd-species in solution by palladium black formation that is supposed to be higher in the case of the Pd/C catalyst given the higher level of metal leaching and the observed palladium aggregation [15].

Table 9: Determination of dissolved Pd, expressed in ppm and % of introduced Pd.

Entry	**Catalyst**	**A_{max} ($mol_{(3a+4a)}/mol_{Pd}/h$)**	**Leaching**		**$A_{max\text{-}cor}$ ($mol_{(3a+4a)}/mol_{leached\text{-}Pd}/h$)^a**
			ppm	**%**	
1	Pd/SiO_2	19	5	0.5	3840
2	Pd/C	33	26	2.7	1260

^{a} $A_{max\text{-}cor}$ = A_{max}/[leached Pd]

Finally, the recycling of the Pd/SiO_2 and Pd/C catalysts was evaluated (Table 10). In order to get accurate results, an initial loading of 6mol% [Pd] was used to have enough catalytic material to perform the tests over several cycles. Regardless the catalysts, for the first run, the results after 1 hour reaction time confirmed the previous experiments, the Pd/C catalyst being more active than the Pd/SiO_2 catalyst (with, resp., 98 and 87 % combined **3a+4a** yield). However, since the second run the behavior changed. While the activity of the Pd/SiO_2 catalyst decreased giving 45% combined yield, it stayed constant over the next two runs. For the Pd/C catalyst, a strong drop of activity was observed since the second run as attested by the limited 23% combined **3a+4a** yield that continued to decrease in the next runs, the catalyst being almost inactive in the third run. These results indicate that, while highly active, the Pd/C catalyst is not recyclable under our reaction conditions.

Table 10: Recycling Pd/C and Pd/SiO_2 catalyst for the decarboxylative cross-coupling reaction of ferulic acid with 4-iodoanisole.

Run	**Yield (3a+4a) (%)**[a]		**Leaching**[b]			
			ppm		(%)	
	Pd/SiO_2	Pd/C	Pd/SiO_2	Pd/C	Pd/SiO_2	Pd/C
1	87	98	3	22	0.16	1.15
2	45	23	3	4	0.16	0.21
3	43	3	2	5	0.10	0.26
4	50	2	7	<3	0.37	0.16

Reaction conditions: ferulic acid (1.75 mmol), aryl iodide (1.5 mmol), [Pd] (6mol%), K_2CO_3 (2 equiv.), NMP (5mL), 130°C. [a] Yields and conversions determined by GC after 1h reaction time. [b] Pd leaching expressed in ppm in the bulk solution and percent ratio to introduced palladium amount.

In order to explain these results, additional analysis of the used catalysts were carried out after four runs. Unfortunately, the remaining potassium salts present at the catalyst surface prevented careful XRD or XPS analyses. TEM was more informative and pictures of used Pd/C catalyst (Figure 10a) showed large Pd aggregates up to 100 nm with an average Pd particle size of 22 nm (standard deviation: 2 nm). Instability of the Pd/C catalyst under the electron beam prevented indexation of the observed particles. These data contrast with those obtained for the fresh Pd/C catalyst (see Figure 5a). Therefore, these data indicate that strong agglomeration occurred during the reaction that could explain the low reusability.

For the used Pd/SiO_2 catalyst, TEM analyses of used catalyst showed Pd particles from 3 to 10 nm with average size of 7 nm with a standard deviation of 1.6 nm (Figure 10b). Therefore, on the contrary to the Pd/C catalyst no agglomeration of palladium particles occurred during the reaction, explaining the higher reusability of this catalyst.

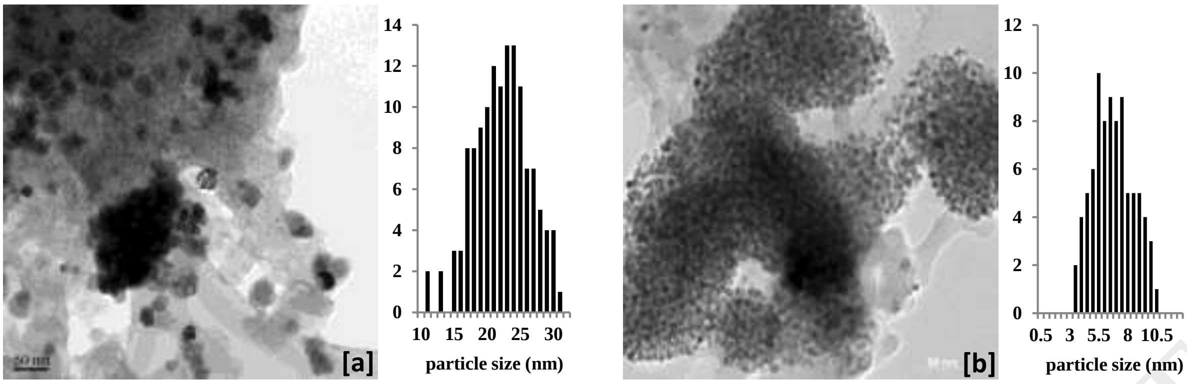

Figure 10: TEM of [a] the Pd/C catalyst after reaction (4 runs) (a) and as received (i.e. fresh) (b) with corresponding histogram of Pd particle size distributions (N = 200) and [b] the Pd/SiO_2 catalyst after reaction (4 runs) with corresponding histogram of PdO particle size distributions (N = 200).

The results observed during the studies could be summarized with the help of Figure 11, in the light of previous literature reports [38, 65, 67]. Whatever the nature of the palladium source (i.e. Pd-salts, Pd/C, Pd/SiO_2), dissolved $Pd^{(0)}$ and/or $Pd^{(II)}$-species, stabilized by coordinated solvent, will be generated in the reaction mixture. These species can undergo to various Pd-materials, active or not. Depending on the palladium concentration in solution these species can form inactive small Pd-particles such as Pd-black. This was observed in few reactions initiated by Pd-salts or with Pd/C heterogeneous catalyst that was evidenced by TEM characterization of used material for the latter (i.e. Figure 10a *versus* Figure 5a). The formation of these species is also a source of catalyst deactivation when using the heterogeneous Pd/C catalyst. Some species, either in native form, or after redox activation, will undergo as $Pd^{(II)}$-catalyst to protodecarboxylation cycle. From our results, this cycle is believed to occur mainly after the Pd-catalyzed Heck-type coupling cycle, which is initiated by Pd^0-species. This assumption is supported by previous publications related to protodecarboxylation of cinnamyl derivatives [38]. However, these species can also undergo to protodecarboxylation prior the Heck-type coupling cycle, delivering in the reaction mixture substituted stilbenes that enter then in classical cross-coupling reaction. This was, for example, believed to occur with ferulic acid that was found to provide easily the corresponding 4-vinylguaiacol **7** under similar reaction conditions [38].

Such reverse order can partially answer to the differences observed in terms of selectivity between products **3** and **4**.

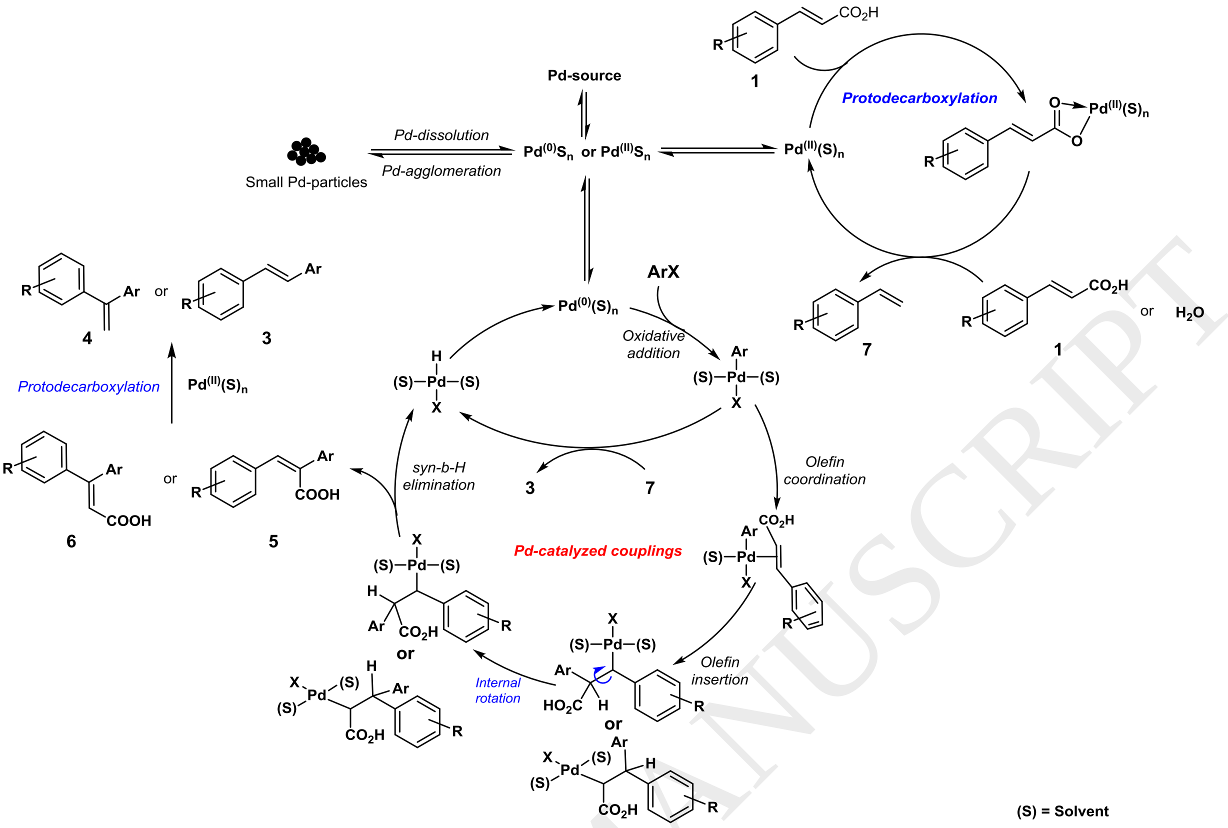

Figure 11: proposed mechanisms in agreement with for the results observed.

4. Conclusion

A procedure for the palladium catalyzed synthesis of stilbenes from cinnamic acid and aryl iodide derivatives was developed. Detailed study showed that, whatever the reaction conditions, two isomers were produced, the expected stilbene and the corresponding 1,1-biphenyl ethylene. After optimization of the reaction conditions, the coupling of ferulic acid and 4-iodoanisole afforded a yield of 78% in the two cross-coupling products with a ratio stilbene/1,1-biphenyl ethylene ≈ 70/30. Developing this procedure to other coupling partners revealed that good yields can be obtained varying the nature of the aryl iodide, but limited possibilities existed when engaging various cinnamic acid derivatives. Here, clearly the main limitation was related to low efficiency of the palladium catalysts to decarboxylate the cinnamic substrates; however, the limitation could be overcome in some cases by adding copper co-catalyst in the reaction mixture following some of our previous reports [38, 65].

For the first time, heterogeneous catalysts (i.e. Pd/C and Pd/SiO$_2$) were engaged in the decarboxylative cross-coupling reaction of ferulic acid and 4-iodoanisole. Both catalysts gave high product yields; however, while the Pd/C catalyst was found to be initially more active than the Pd/SiO$_2$ catalyst it led to strong deactivation since the second reuse due to high rate of palladium leaching during the first run and strong agglomeration of the Pd-particles. On the contrary the Pd/SiO_2 catalyst, while leading as well to some deactivation, could be reused over at least 4 cycles.

Acknowledgements

The authors gratefully acknowledge the National Agency of Research (CHEMLIVAL N° ANR-12-CDII-0001_01) for funding. N.R. thanks the Ministry of Research and Education for grant.

References

[1] J.A. Baur, D.A. Sinclair, Nat. Rev. Drug. Discov. 5 (2006) 493-506.
[2] M.-H. Pan, G. Ghai, C.-T. Ho, Mol. Nutr. Food Res. 52 (2008) 43-52.
[3] T. Eicher, S. Fey, W. Puhl, E. Büchel, A. Speicher, Eur. J. Org. Chem. (1998) 877-888.
[4] Y. Kosenkova, M. Polovinka, N. Komarova, D. Korchagina, N. Kurochkina, V. Cheremushkina, N. Salakhutdinov, Chem. Nat. Compnd. 43 (2007) 712-713.
[5] S. Friederich, U.H. Maier, B. Deus-Neumann, Yoshinori Asakawa, M. H. Zenk, Phytochem. 50 (1999) 589-598.
[6] L. Fang, H.-F. Guo, H.-X. Lou, Helv. Chim. Acta. 90 (2007) 748-752.
[7] K. Ferré-Filmon, L. Delaude, A. Demonceau, A.F. Noels, Coord. Chem. Rev. 248 (2004) 2323-2336.
[8] K.B. Becker, Synthesis. 1983 (1983) 341-368.
[9] G.I. Likhtenshtein, Stilbenes Applications in Chemistry, Life Sciences and Materials Science, Wiley-VCH, 2010, pp. 1-25.
[10] M.B. Andrus, J. Liu, E.L. Meredith, E. Nartey, Tetrahedron Lett. 44 (2003) 4819-4822.
[11] L. Botella, C. Nájera, Tetrahedron. 60 (2004) 5563-5570.
[12] M.B. Andrus, J. Liu, Tetrahedron Lett. 47 (2006) 5811-5814.
[13] A. Farina, C. Ferranti, C. Marra, Nat. Prod. Res. 20 (2006) 247-252.
[14] M. Gruber, S. Chouzier, K. Koehler, L. Djakovitch, Appl. Catal. A: Gen. 265 (2004) 161-169.
[15] L. Djakovitch, K. Koehler, J.G. De Vries, in: D. Astruc (Ed.), Nanoparticles and Catalysis., Wiley-VCH, Weinheim, 2008, pp. 303-348.
[16] M.J. Climent, A. Corma, S. Iborra, M. Mifsud, Adv. Synth. Catal. 349 (2007) 1949-1954.
[17] L. Joucla, G. Cusati, C. Pinel, L. Djakovitch, Tetrahedron Lett. 49 (2008) 4738-4741.
[18] L. Joucla, G. Cusati, C. Pinel, L. Djakovitch, Appl. Catal. A: Gen. 360 (2009) 145-153.
[19] L. Joucla, G. Cusati, C. Pinel, L. Djakovitch, Adv. Synth. Catal. 352 (2010) 1993-2001.
[20] M.S. Kabir, A. Monte, J.M. Cook, Tetrahedron Lett. 48 (2007) 7269-7273.
[21] V. Kogan, Z. Aizenshtat, R. Popovitz-Biro, R. Neumann, Org. Lett. 4 (2002) 3529-3532.
[22] J.-H. Li, X.-C. Hu, Y. Liang, Y.-X. Xie, Tetrahedron. 62 (2006) 31-38.
[23] A.G. Myers, D. Tanaka, M.R. Mannion, J. Am. Chem. Soc. 124 (2002) 11250-11251.
[24] S.-L. Zhang, Y. Fu, R. Shang, Q.-X. Guo, L. Liu, J. Am. Chem. Soc. 132 (2009) 638-646.
[25] P. Hu, J. Kan, W. Su, M. Hong, Org. Lett. 11 (2009) 2341-2344.
[26] Z. Fu, S. Huang, W. Su, M. Hong, Org. Lett. 12 (2010) 4992-4995.
[27] Y. Zhao, Y. Zhang, J. Wang, H. Li, L. Wu, Z. Liu, Synlett. 2010 (2010) 2352-2356.
[28] J. Wang, Z. Cui, Y. Zhang, H. Li, L.-M. Wu, Z. Liu, Org. Bio. Chem. 9 (2011) 663-666.
[29] F. Jafarpour, S. Zarei, M. Barzegar Amiri Olia, N. Jalalimanesh, S. Rahiminejadan, J. Org. Chem. 78 (2013) 2957-2964.
[30] L.J. Goossen, G. Deng, L.M. Levy, Science. 313 (2006) 662-664.
[31] L.J. Goossen, N. Rodriguez, B. Melzer, C. Linder, G. Deng, L.M. Levy, J. Am. Chem. Soc. 129 (2007) 4824-4833.
[32] G. Cahiez, A. Moyeux, M. Poizat, Chem. Commun. 50 (2014) 8982-8984.
[33] J. Tang, D. Hackenberger, L.J. Goossen, Angew. Chem. Int. Ed. 55 (2016) 11296-11299.

[34] M. Yamashita, K. Hirano, T. Satoh, M. Miura, Chem. Lett. 39 (2010) 68-69.

[35] Z. Wang, Q. Ding, X. He, J. Wu, Org. Bio. Chem. 7 (2009) 863-865.

[36] X. Wang, S.-y. Li, Y.-m. Pan, H.-s. Wang, Z.-f. Chen, K.-b. Huang, J. Org. Chem. 80 (2015) 2407-2412.

[37] A. Shard, N. Sharma, R. Bharti, S. Dadhwal, R. Kumar, A.K. Sinha, Angew. Chem. Int. Ed. 51 (2012) 12250-12253.

[38] S. Cadot, N. Rameau, S. Mangematin, C. Pinel, L. Djakovitch, Green Chem. 16 (2014) 3089-3097.

[39] B. Bartolomé, C. Gómez-Cordovés, J. Sci. Food Agric. 79 (1999) 435-439.

[40] D. Hernanz, V. Nuñez, A.I. Sancho, C.B. Faulds, G. Williamson, B. Bartolomé, C. Gómez-Cordovés, J. Agric. Food Chem. 49 (2001) 4884-4888.

[41] M.M. Pedrosa, M. Muzquiz, C. García-Vallejo, C. Burbano, C. Cuadrado, G. Ayet, L.M. Robredo, J. Sci. Food Agric. 80 (2000) 459-464.

[42] K.-H. Kim, R. Tsao, R. Yang, S.W. Cui, Food Chem. 95 (2006) 466-473.

[43] H.J. Park, K.-H. Park, J.-K. Jeon, J. Kim, R. Ryoo, K.-E. Jeong, S.H. Park, Y.-K. Park, Fuel. 97 (2012) 379-384.

[44] J. Tarabay, W. Al-Maksoud, F. Jaber, C. Pinel, S. Prakash, L. Djakovitch, Appl. Catal. A: Gen. 388 (2010) 124-133.

[45] V.M. Bhusainahalli, C. Spatafora, M. Chalal, D. Vervandier-Fasseur, P. Meunier, N. Latruffe, C. Tringali, Eur. J. Org. Chem. 2012 (2012) 5217-5224.

[46] J. Hitce, M. Crutizat, C. Bourdon, A. Vives, X. Marat, M. Dalko-Csiba, Green Chem. 17 (2015) 3756-3761.

[47] F. Bertaud, J.P. Croue, B. Legube, Ozone: Sci. Eng. 23 (2001) 139-148.

[48] A. Sharma, N. Sharma, R. Kumar, U.K. Sharma, A.K. Sinha, Chem. Commun. (2009) 5299-5301.

[49] R.I. Campos, X. Wu, M. Elgland, P. Konradsson, P. Hammarstroem, ACS Chem. Neurosci. 7 (2016) 924-940.

[50] M. Chalal, D. Vervandier-Fasseur, P. Meunier, H. Cattey, J.-C. Hierso, Tetrahedron. 68 (2012) 3899-3907.

[51] Z. Li, K. Wu, G. Su, Y. He, Opt. Mater. 20 (2002) 295-299.

[52] L. Djakovitch, K. Koehler, J. Am. Chem. Soc. 123 (2001) 5990-5999.

[53] L. Djakovitch, H. Heise, K. Köhler, J. Organomet. Chem. 584 (1999) 16-26.

[54] A.K. Shil, P. Das, RSC Adv. 5 (2015) 24859-24863.

[55] Z. Chen, M. Luo, Y. Wen, G. Luo, L. Liu, Org. Lett. 16 (2014) 3020-3023.

[56] M.K. Karunananda, N.P. Mankad, J. Am. Chem. Soc. 137 (2015) 14598-14601.

[57] X.-D. Xiao, Y.-L. Bai, J.-Q. Liu, J.-W. Wang, Tetrahedron Lett. 57 (2016) 3385-3388.

[58] G. Valdameri, L. Pereira Rangel, C. Spatafora, J. Guitton, C. Gauthier, O. Arnaud, A. Ferreira-Pereira, P. Falson, S.M.B. Winnischofer, M.E.M. Rocha, C. Tringali, A. Di Pietro, ACS Chem. Biol. 7 (2012) 322-330.

[59] V.P. Androutsopoulos, K.C. Ruparelia, A. Papakyriakou, H. Filippakis, A.M. Tsatsakis, D.A. Spandidos, Eur. J. Med. Chem. 46 (2011) 2586-2595.

[60] J.G. Cole, P. Wan, Can. J. Chem. 80 (2002) 46-54.

[61] A. Arcadi, S. Cacchi, F. Marinelli, Tetrahedron Lett. 27 (1986) 6397-6400.

[62] A. Gavryushin, C. Kofink, G. Manolikakes, P. Knochel, Tetrahedron. 62 (2006) 7521-7533.

[63] A. Gordillo, E. de Jesus, C. Lopez-Mardomingo, Chem. Commun. (2007) 4056-4058.

[64] M.-Y. Chang, Y.-H. Huang, H.-S. Wang, Tetrahedron. 72 (2016) 3022-3031.

[65] N. Rameau, S. Cadot, A. Paquet, C. Pinel, L. Djakovitch, Top Catal. 57 (2014) 1430-1437.

[66] A.H.M. de Vries, J.M.C.A. Mulders, J.H.M. Mommers, H.J.W. Henderickx, J.G. de Vries, Org. Lett. 5 (2003) 3285-3288.

[67] N. Rodriguez, L.J. Goossen, Chem. Soc. Rev. 40 (2011) 5030-5048.

[68] J.D. Weaver, A. Recio, A.J. Grenning, J.A. Tunge, Chem. Rev. 111 (2011) 1846-1913.

[69] G.J.P. Perry, I. Larrosa, Eur. J. Org. Chem. 2017 (2017) 3517-3527.

[70] X. Qin, C. Chen, L. Zhang, J. Xu, Y. Pan, H. Zhao, J. Han, H. Li, L. Xu, Tetrahedron. 73 (2017) 2242-2249.
[71] K. Köhler, R.G. Heidenreich, J.G.E. Krauter, J. Pietsch, Chem. Eur. J. 8 (2002) 622-631.
[72] R.G. Heidenreich, K. Köhler, J.G.E. Krauter, J. Pietsch, Synlett (2002) 1118-1122.
[73] A.K. Zharmagambetova, V.A. Golodov, Y.P. Saltykov, J. Mol Catal. 55 (1989) 406-414.
[74] K.-T. Li, M.-H. Hsu, I. Wang, Catal. Commun. 9 (2008) 2257-2260.
[75] L. Djakovitch, P. Rollet, Adv. Synth. Catal. 346 (2004) 1782-1792.
[76] P. Rollet, W. Kleist, V. Dufaud, L. Djakovitch, J. Mol Catal. A: Chem. 241 (2005) 39-51.
[77] M. Genelot, V. Dufaud, L. Djakovitch, Adv. Synth. Catal. 355 (2013) 2604-2616.
[78] M. Wagner, K. Köhler, L. Djakovitch, S. Weinkauf, V. Hagen, M. Muhler, Top. Catal. 13 (2000) 319-326.
[79] L. Djakovitch, M. Wagner, C.G. Hartung, M. Beller, K. Koehler, J. Mol. Catal. A: Chem. 219 (2004) 121-130.
[80] G. Collins, M. Schmidt, C. O'Dwyer, G. McGlacken, J.D. Holmes, ACS Catalysis. 4 (2014) 3105-3111.